Climate Modelling User Group

Phase 2 Deliverable 4.1   Version 3

MIP Impact Assessment

Centres providing input: SMHI, IC3/BSC, MétéoFrance

Version nr.	Date	Status
0.6	06 May 16	Input from partners
2.6	18 Jun 17	Additional contribution from CNRM and BSC and update of the whole document
3.0	30 Jun 17	Submit to ESA

CMUG Phase 2 Deliverable 4.1

MIP Impact Assessment

Table of Contents

MIP Impact Assessment Report

1. Purpose and scope of this report

The purpose of this document is to describe the quality relevant outcomes from the research of Work Packages 4.1, 4.2 and O4.2, entitled "Exploiting CCI products in CMIP like experiments" after three years of activity within the CMUG Phase 2 project.

The activity of this work package consists in assessing the impact of using CCI data records as surface boundary fields for AMIP simulations to establish a test case that illustrates the impact of CCI data records (SST and sea ice) on AMIP-like simulations (also called CCI4MIP simulations). As part of the activity of this Work Package, the same CCI data records were also used as reference data sets for the evaluation of high resolution seasonal forecast simulations. Some of the scientific questions addressed originally in this work package are:

- Is there an added value on the representation of mean climate and its variability, in particular at higher latitudes, from the CCI data set compared with AMIPII SST and sea ice concentration (SIC) boundary conditions?
- Is this added value better identified in high resolution simulations of the atmospheric model (with a resolution of about 50km compared to about 150km)?
- How do the prediction scores of high resolution seasonal forecast vary when using the CCI SST and sea ice concentrations as reference data sets compared to other commonly used reference data sets ?

2. Methodology and approach

To assess the impact of using CCI data records as surface boundary fields for AMIP simulations, a test case illustrating the impact of CCI data records on AMIP simulations was established. The required tasks consisted in:

1) Preparing and analysing boundary conditions for global AMIP simulations using CCI-data records (SST and sea ice concentration).
2) Performing CCI4AMIP simulations with the two different resolution versions of an atmospheric climate model.
3) Quantifying and reporting the impact of using CCI data sets on AMIP model simulations.

SMHI contributed to this activity through the analysis of the CCI SIC v1 (see Section 3.1). Météo-France/CNRM contributed to the activity through an assessment of CCI SIC v2 (see Section 3.2) and CCI4MIP simulations using the atmosphere general circulation model ARPEGE-Climat as part of the CNRM-CM coupled ocean-atmosphere general circulation

CMUG Phase 2 Deliverable

Reference:	D4.1: MIP Impact Assessment
Due date:	30 June 2017
Submission date:	30 June 2017
Version:	3

model (see Section 4). Simulations were done with a new version of the model developed in preparation to the CMIP6 simulations exercise. Two model resolution were used consistently with those used in CMIP6 : T127 (1.4°x1.4°) for the lowest (see Section 4.1) and T359 (0.5°x0.5°) for the highest (see Section 4.2).

Contrary to CMIP experiments, the overall objective of this simulation exercise is not to first compare different model performances, but to analyse the impact of using CCI data sets as boundary conditions compared to using the classical AMIP forcing (Taylor et al. 2015, also described in Hurrel et al. 2008 and available at https://pcmdi.llnl.gov/mips/amip/) applied in a coherent way. Some of the experiments were made before the final CCI SIC data sets are available and for a shorter period than the existing CMIP5 AMIP boundary fields (several decades). Being in between CMIP5 and CMIP6 intercomparison exercises, Météo-France used a model version that was not run for CMIP5. However, the model versions (low and high resolution ones) are close to the final one to be used for CMIP6. This implies in particular that new specific reference simulations with the classical AMIP forcing had to be performed to allow the comparison with the CCI4MIP simulations.

Another aim of these experiments was to demonstrate the practical use of CCI SST and Sea Ice data and to prepare this data so it can readily be used by other model groups. Since the final CCI data sets are now available, their use in this CCI4MIP exercise in one institute demonstrates their applicability to other institutes for such a kind of modelling exercise.

As part of the evaluation of high resolution seasonal forecasts, the main task consisted in evaluating the model climatology and seasonal forecast skill when using either the CCI SST as reference data sets or data sets that are currently used as ERA-Interim reanalysis (Dee et al., 2011), the NOAA Extended Reconstructed Sea Surface Temperature v3b (Smith et al., 2007; hereafter referred to as ERSST) or the Hadley Sea Surface data set (Rayner et al., 2003; hereafter referred to as HadSST).

IC3/BSC validated against the CCI SST data set, a set of very high resolution (ORCA025L75 – T511L91) EC-Earth3 seasonal forecasts: 10-member predictions initialized every 1st November and 1st May from the GLORYS2v1 and ERA-Interim reanalyses and run for 4 months into the future. Due to the problems encountered with the version v1 of the CCI SIC (see Section 3.1), only the CCI SST was used in this assessment exercise.

The overall objective of this exercise was to evaluate the possible added-value on forecast skill scores when using the CCI SST as a reference data set compared to other commonly used reference data sets (see Section 5.1). The information on the uncertainty given with the CCI products was also exploited in order to identify what are the main sources of uncertainty in the forecast skill scores (see Section 5.2).

3. CCI Data analysis

3.1   Assessment of CCI SIC version v1

Within the context of the preparation of the CC4MIP simulation exercise, SMHI performed an analysis of the CCI data sets. The original CCI SIC product (25 km EASE-grid) in its first version (CCI SIC v1), the CCI SSTv1 and OSTIA sea ice data (0.05 lon-lat grid) were interpolated to a common regular 0.25x0.25 lon-lat grid in order to compare the ice results, investigate possible inconsistencies between the CCI sea ice product and the SST-product and have them easy available as possible forcing data. The common available period from 1992-2008 was used. Furthermore, NOAA-OISST (at 0.25 degree grid) was used as comparison. Figure 3.1 shows substantial differences between the CCI sea ice concentration and the NOAA-data. Generally, the ice extent in CCI is smaller in March. This is even more pronounced in the Antarctic (not shown). However, daily variations of the differences are large and an example from the record-low sea ice extent in September 2007 shows smaller ice extent in the CCI dataset (Figure 3.2)
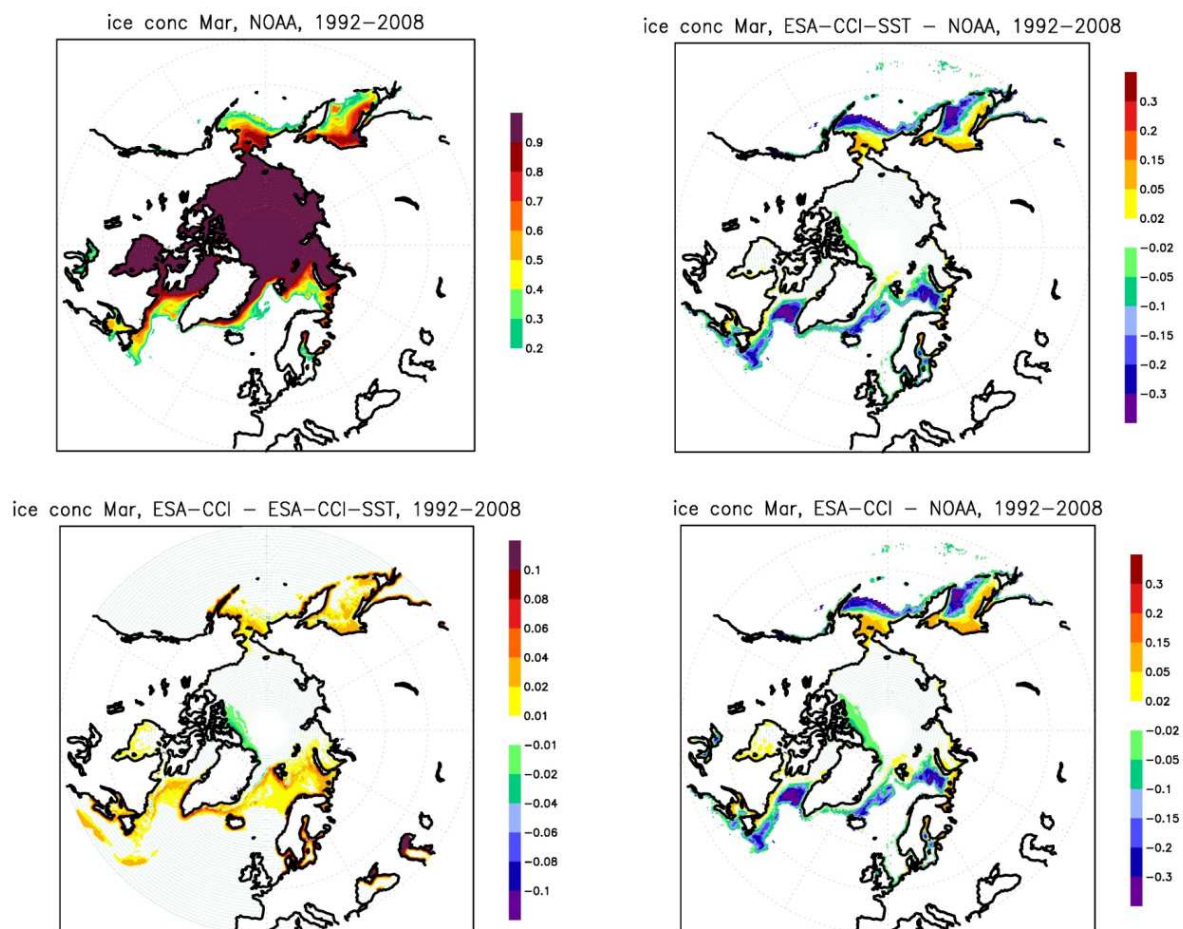

Figure 3.1: March sea ice concentration in the NOAA-OISST sea ice data averaged over 1992-2008 (top left), difference between ice concentration in CCI and OSTIA (bottom left), difference between OSTIA and NOAA (top right) and difference between CCI and NOAA.
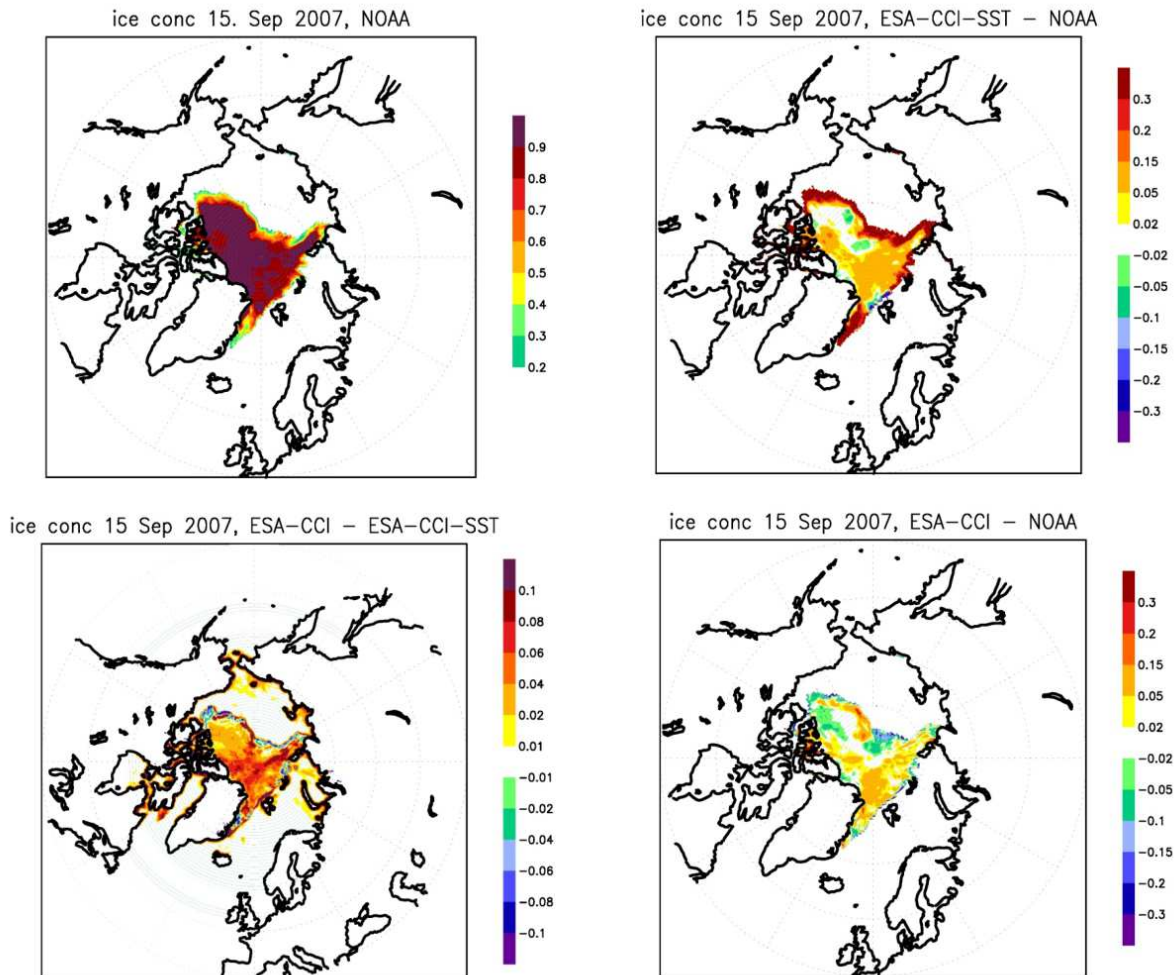
Figure 3.2 : As Figure 3.1 but for sea ice concentration at 15th September 2007.

Obviously, it is unclear which of the data sets is more reliable but differences among different ice data are large indicating large uncertainties in the satellite data products. These results confirm earlier results which found substantial ice concentration differences between other existing satellite derived sea ice data sets.

SMHI further compared CMIP5 sea ice concentrations to satellite data and found that depending on the data set used, different conclusions about the performance of the models are drawn. This makes evaluation and improvement of climate models extremely challenging.

Analyses at SMHI of daily sea ice concentration CCI data showed the occurrence of unrealistic sea ice concentrations far away from the Arctic or areas where sea ice could be expected (Figure 3.3). Ice concentrations up to 15% occur in such regions. Using these data as lower boundary forcing for AGCM-simulations will lead to huge unrealistic ocean to atmosphere heat fluxes. It was thus considered that it does not make sense to perform any AGCM-simulations using the new CCI ice concentration from the CCI SIC v1. It was thus

decided to perform the first CCI4MIP simulations to test only the impact of the CCI-SST (see Section 4.1) expecting a new version of the CCI SIC before performing a new test.
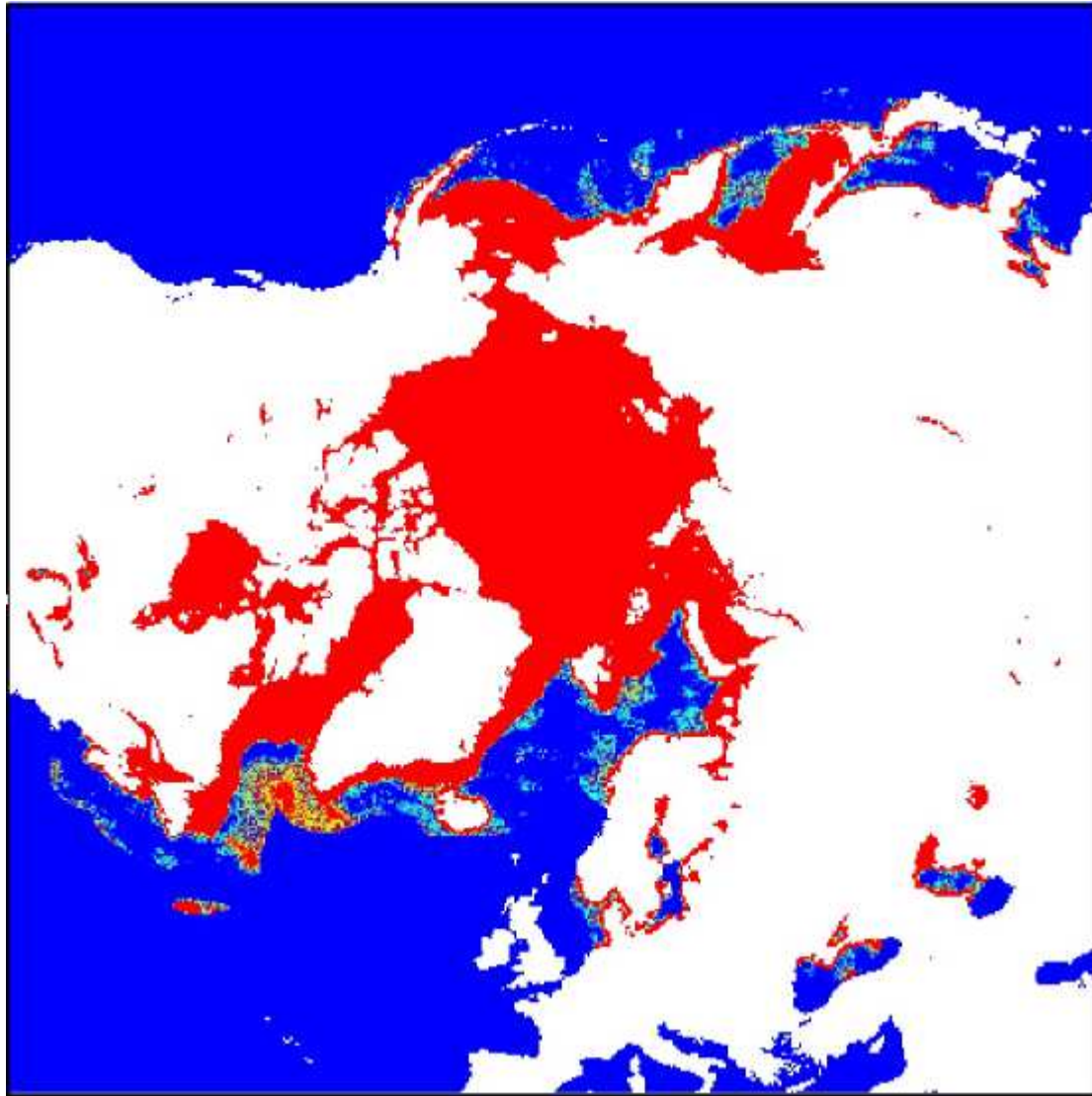

Figure 3.3: Example for occurrence of unrealistic sea ice concentrations in ESA-CCI ice concentration data set (range of concentration of sea ice from 0 to 5%).

3.2   Assessment of CCI SIC version v2

A second version of the CCI SIC dataset became available in January 2017. An interaction with the Sea Ice team allowed recovering the dataset before its public release in March. According to the Sea Ice team, the problems encountered with the CCI SIC v1 were solved through the application of a data filtering process to produce the main product of the L4 dataset (Sørensen and T. Lavergne, 2017). The L4 variables were produced at two different resolutions (25km and 50km) but only the higher resolution filtered variable was used at Météo-France for one CCI4MIP simulation (see Section 4.2). The choice of the higher

CMUG Phase 2 Deliverable

Reference:	**D4.1: MIP Impact Assessment**
Due date:	**30 June 2017**
Submission date:	**30 June 2017**
Version:	**3**

resolution was guided by the fact that the version of the Arpege-climat model used for this simulation (T359 model version) has a grid cell size much lower than 50km at higher latitudes.

As part of the CCI data analysis, the CCI SIC v2 dataset was compared to the classical AMIP sea ice dataset. This comparison was performed by analysing the difference between CCI SIC and AMIP SIC averaged for January and October over the whole CCI4MIP simulation period (2003-2010) and on the model grid (Figure 3.4). The CCI SIC shows generally weaker concentrations than SIC AMIP in Northern Hemisphere as shown for January and October (top figures). This is mainly the case over the marginal ice zone were the differences may reach about 10%. Even if one part of the explanation might be that the filtering may remove some true ice coverage (Sørensen and T. Lavergne, 2017) this appears to be the main difference between the two products.
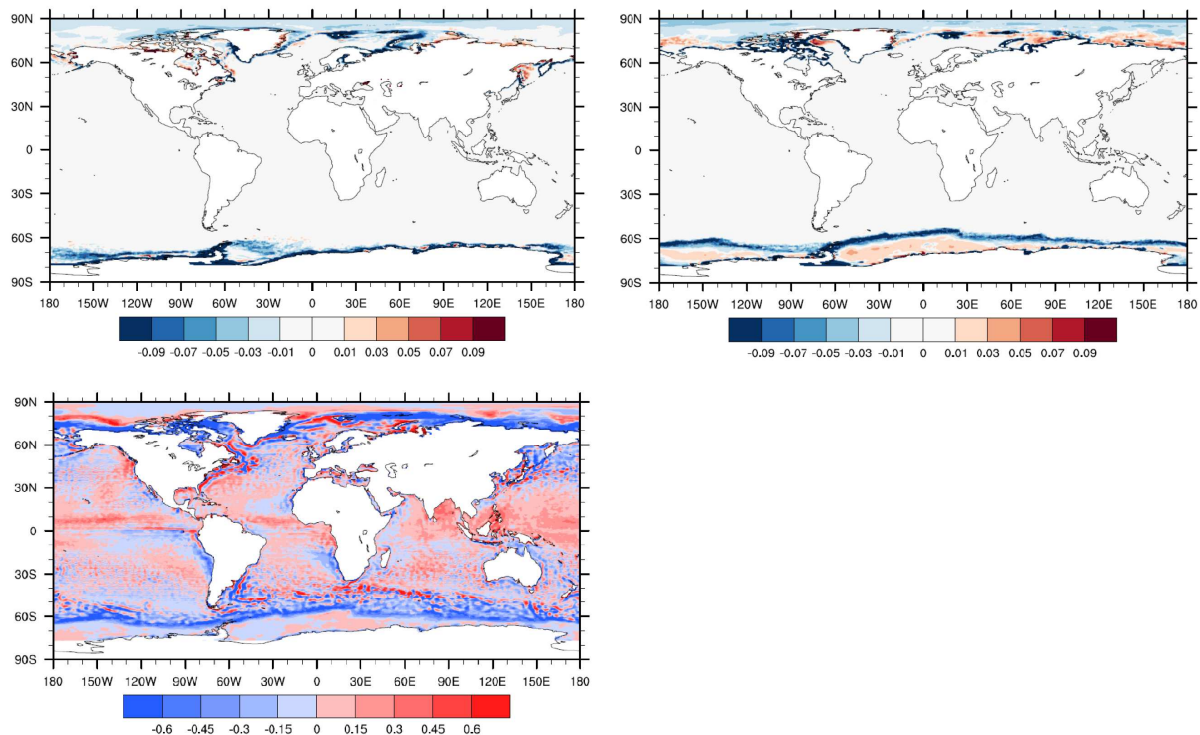

Figure 3.4: Sea ice concentration (SIC) difference between the CCI4MIP and AMIP (T359 model version) simulations for the climatology averaged over 2003-2010 of January (top left) and October (top right); SST difference between the CCI4MIP and AMIP (T359 model version) in October. (bottom).

For October, we have also reproduced in Figure 3.4 the SST mean differences between CCI and AMIP (bottom Figure). In the Antarctic marginal ice zone this is unexpected since lower SIC in this zone should result in higher temperatures. This could be explained by the definition of sea ice concentration in the SST CCI product that differs from SIC CCI as it is sourced on Norwegian Met Office's OSISAF products (Merchant and Spink, 2013). This needs further investigation.

CMUG Phase 2 Deliverable

Reference:	**D4.1: MIP Impact Assessment**
Due date:	**30 June 2017**
Submission date:	**30 June 2017**
Version:	**3**

4. Impact in AMIP simulations

4.1 Assessment of the impact of CCI SST

Due to the delay in the sea ice data delivery (see previous Section), the first AGCM AMIP-like simulations were performed in order to assess the impact of the CCI SST only.

At Météo-France (CNRM) two 5-member ensembles of simulations were performed with a new version of the Arpege-Climat model. The model version has been chosen as close as possible to the atmospheric component of the CNRM-CM coupled model that will be used for the CMIP6 international simulation exercise. It includes a new physical package compared to the CNRM-CM5 atmospheric component used for CMIP5 (Voldoire et al., 2013), but this version needs further parameter adjustments coming from its evaluation in a full coupled mode. The resolution here chosen corresponds to the lowest of the two resolutions that have been selected by CNRM and CERFACS for their CMIP6 simulations. It consists in a T127 spectral truncation (about 1.4° in latitude and longitude) with 91 vertical levels.

The first ensemble (hereafter referred to as AMIP) was performed using the SST and Sea ice extent currently used by climate scientists to perform the AMIP simulations. The SST is thus the one provided by Taylor et al. (2015). In the second ensemble of simulations (hereafter referred to as CCI4MIP), this SST was replaced by the CCI SST interpolated on the model grid and averages at the monthly time scale in agreement with the "standard" AMIP forcing. The Sea Ice extent dataset used to constrain the model remains the same than the "standard" dataset used for the AMIP simulations. To account for the longest period covered with the CCI dataset (L4, v1.0), the common analysis period extends from 1992 to 2010.

CMUG Phase 2 Deliverable

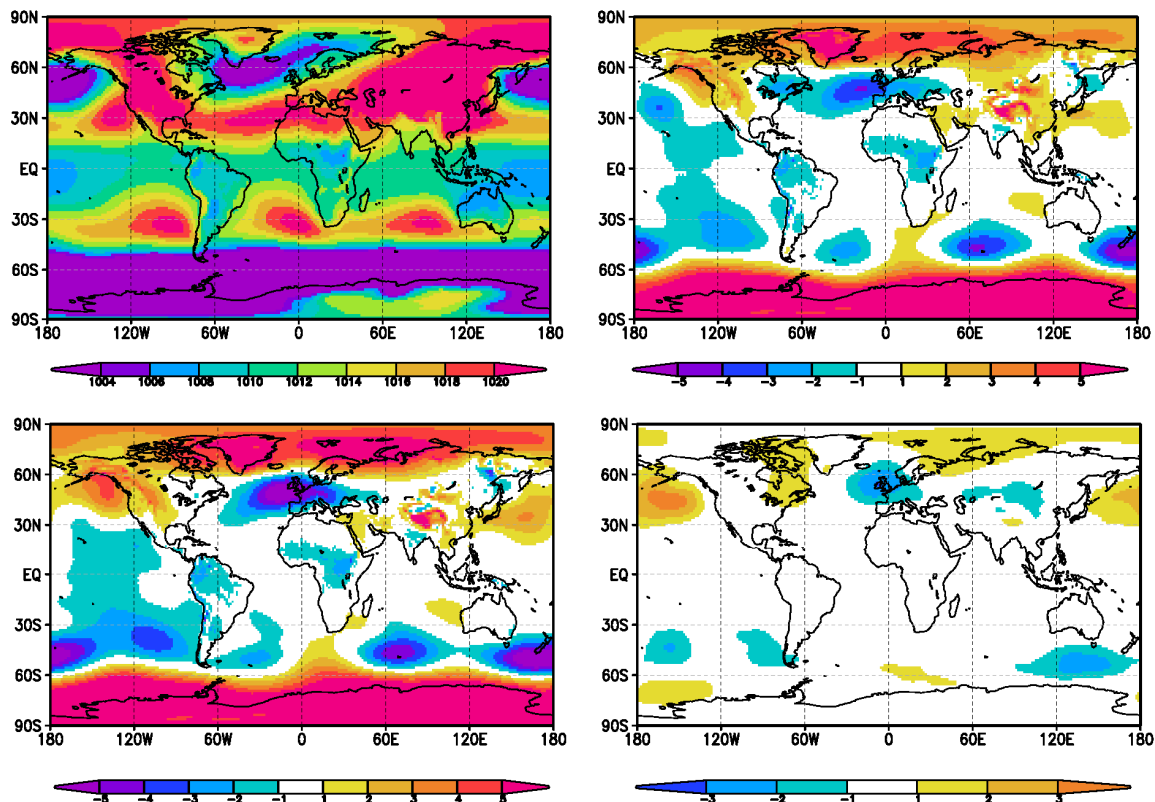|	
Reference:	**D4.1: MIP Impact Assessment**
Due date:	**30 June 2017**
Submission date:	**30 June 2017**
Version:	**3**

Figure 4.1: Sea level pressure in December-January-February averaged over the 1992-2010 period (in hPa) : ERA-Interim climatology (top left), difference between one member of the AMIP ensemble and Era-Interim (top right), difference between one member of the AMIP ensemble and ERA-Interim (bottom left), difference between the two chosen members of the CCI4MIP and AMIP ensembles of simulations (bottom right).

The difference between the two ensembles is illustrated in Figure 4.1 showing the model biases compared to ERA-Interim climatology for the mean sea-level pressure in Northern hemisphere winter (DJF) for the 1992-2010 period. We have here selected one member in each of the 5-member ensembles. The model biases are slightly degraded when using the CCI forcing rather than the AMIP forcing, since the root mean square difference between the model and the climatology increases from 2.22 hPa to 2.48 hPa. This degradation comes in particular from an accentuation of the negative pressure biases over North-Eastern Atlantic and Western Europe that leads to a too zonal circulation in this region.

In this analysis we found a special case that is August 2006 (Figure 4.2) showing a slight SST difference of about 0.2 K. This difference has a significant (at 5% level) impact on the precipitation (within about 10%) over Western Tropical Pacific according to a student's t_test. This region is known to have large climate sensitivity to SST changes trough the convection intensification over warmer waters.

For a better understanding of the precipitation variation related to the SST changes the differences are computed also for the climatology averaged over the simulation period and the 5-member ensembles for the months of January and July (Figure 4.3) for SST and precipitation. In January as in July the CCI SST is a few tenths of a degree higher than AMIP

CMUG Phase 2 Deliverable

Reference:	**D4.1: MIP Impact Assessment**
Due date:	**30 June 2017**
Submission date:	**30 June 2017**
Version:	**3**

SST over inter-tropical regions and colder at mid-latitudes. The intertropical pattern of change is correlated with a corresponding pattern of precipitation change with higher precipitation particularly over the Warm Pool region (Figure 4.3 top left and bottom left). This finding is in agreement with the results of Palmer and Mansfield (1984) and the more recent results of Barsugli and Sardeshmukh (2002) about the impact of the SST changes on the precipitation in Western Tropical Pacific. In this last study, the estimated local precipitation sensitivity to SST change of about 0.5 mm day^{-1} K^{-1} over Western Tropical Pacific is consistent with our finding of a precipitation change of about 1 mm day^{-1} associated to a SST change of about 0.2 K. Colder temperatures over the Indian Ocean might also be linked to the specific pattern of precipitation change of the Indian monsoon (lower over the western coast of India and enhanced over the inland regions of the country).
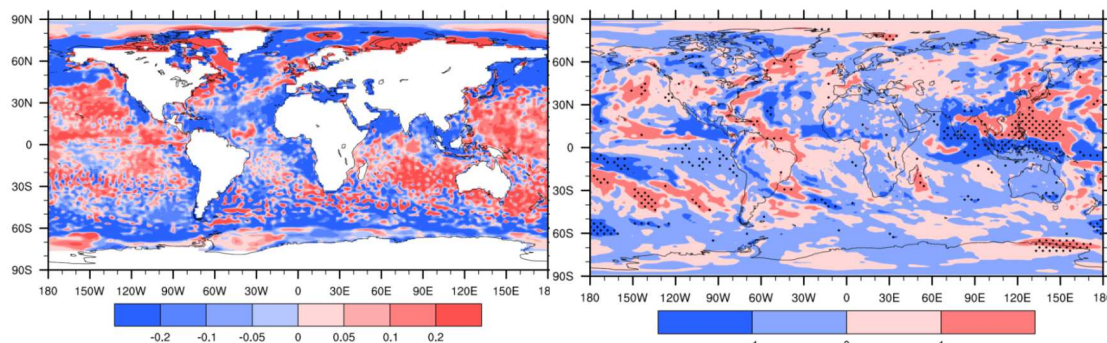

Figure 4.2: SST (left) and precipitation (right) differences (respectively in K and mm day^{-1}) between the CCI4MIP and AMIP (T127model version) ensembles of simulations in August 2006, calculated as an average over the 5-members of each ensemble. Doted zones correspond to regions where the 5% level of significance is over-passed in the application of a student t-test.
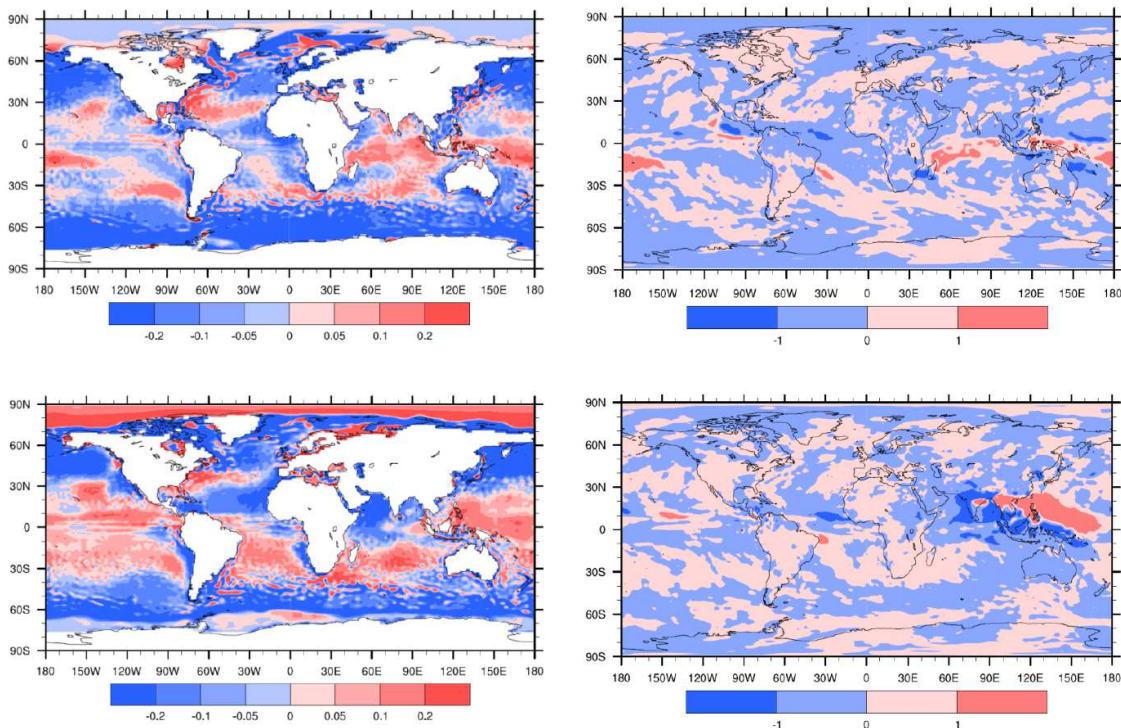

Figure 4.3 : SST (left) and precipitation (right) differences (respectively in K and mm day^{-1}) between the CCI4MIP and AMIP (T127) ensembles for the climatology of January (top) and of July (bottom), calculated as an average over the 5-members of each ensemble.

4.2   Assessment of the impact of CCI SIC

Additionally a CCI4MIP one member simulation was run with the higher resolution version of Arpege-Climat (T359 or about 0.5°, close to that will be used for CMIP6) using the CCI SST (L4 v1.1; monthly means) and the CCI SIC (L4 filtered v2.0; monthly means at 25km) boundary conditions over the common period 2003-2010 of the two forcing datasets. The simulation was compared with a control AMIP simulation performed with the same model version over the same period.

We have reported in Figure 4.4 differences between the CCI4MIP and AMIP simulations and, for the sake of comparison, those obtained with only one member of the CCI4MIP and AMIP ensembles of simulations performed with the lower resolution of the model (T127) and presented in the previous Section.

The SST patterns of differences between CCI and AMIP averaged over the 2003-2010 period are very similar for the two model versions in July (Figure 4.4, left), even if it is of course smoother with the T127 model version. This is also confirmed for all the monthly averages. This occurs in spite of the fact that the two versions of the climate model were forced with different versions of the CCI SST (v1.0 and v1.1). But according to the CCI SST team, only "intermittent bugs in the externally sourced sea ice fields (with corresponding implications for high latitude SST) have been corrected" with little impact and only at the higher latitudes. The common pattern of change exhibits some persistent small scale structure (also persistent from month to month) that could be related to the interpolation process ("Gibbs effect").

Regarding the precipitation differences (Figure 4.4, right), they are a little bit more pronounced. However, the locations of these differences are very similar in the two versions in spite of some differences in some details that could be related to climate internal variability. The forced response is the same in the two simulations with the previously mentioned local response of precipitations over the Warm Pool region and an impact on the summer monsoon.
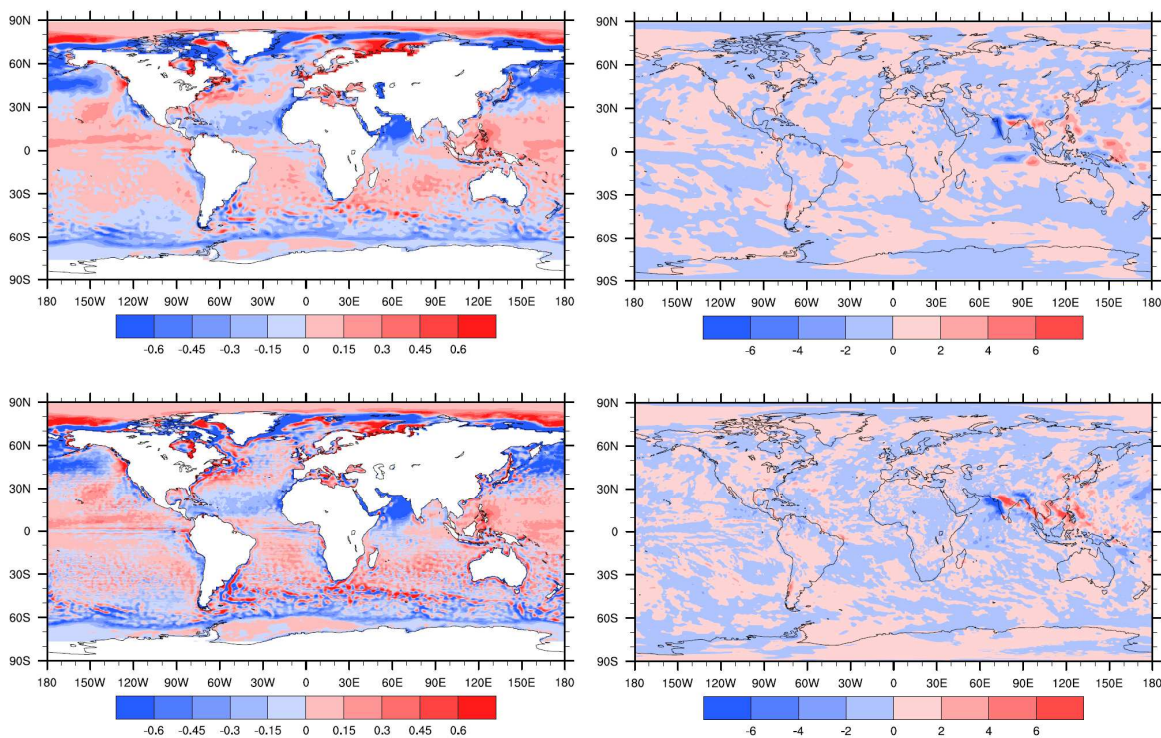
CMUG Phase 2 Deliverable

Reference:	**D4.1: MIP Impact Assessment**
Due date:	**30 June 2017**
Submission date:	**30 June 2017**
Version:	**3**

Figure 4.4: SST (left) and precipitation (right) differences (respectively in K and mm day^{-1}) between the CCI4MIP and AMIP simulations for the climatology of July averaged over 2003-2010 for one member simulation of the T127 model version (top) and for the T359 model version (bottom).

We have reproduced in Figure 4.5 the Z500 hPa differences between the CCI4MIP and the AMIP simulations using the T359 model version and averaged in January over the 2003-2010 period. The pattern is characterized by an increase of the geopotential over the northern polar region accompanied with a decrease in different zones of the surrounding latitudes. This pattern is consistent with a teleconnexion with the western tropical Pacific region consisting in the propagation of stationary Rossby Waves from the warmed western tropical Pacific (Palmer and Mansfield 1984). The same kind of teleconnexion can be inferred from a study of the winter atmospheric response to different patterns of SSTs (Révelard 2017). We thus argue that the atmospheric response is not here the result of the small differences in sea ice concentration between the CCI4MIP and AMIP simulations presented in Figure 3.4 (top left). We also investigated other climate variables in January and found in particular a warmer northern polar region and colder high latitude northern hemisphere continental regions in consistency with higher sea level pressure. Here also, we can argue that the main part of the differences comes from the teleconnection with the tropical region. A complete demonstration would however require further investigation.
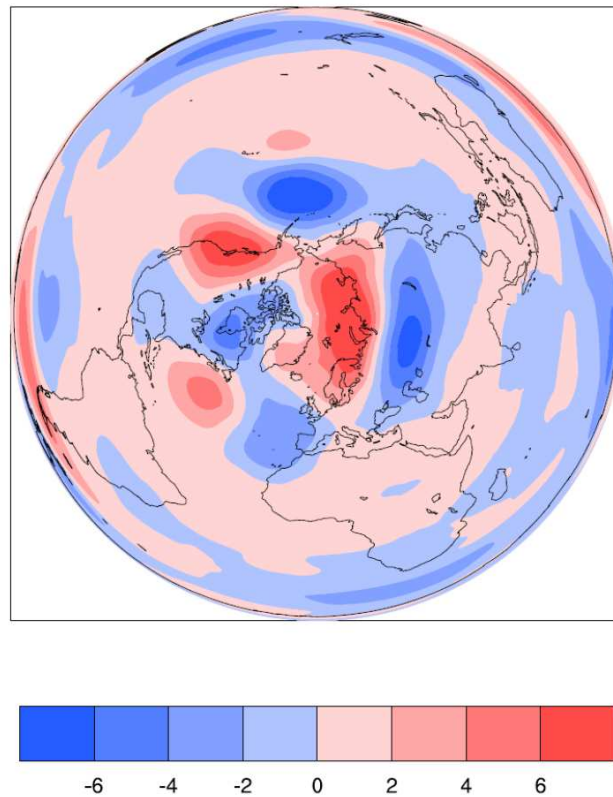
Figure 4.5: Z500 differences (in m) between the CCI4MIP and AMIP simulations for the climatology of January averaged over 2003-2010 and for the T359 model version.

5. Impact in seasonal forecast simulations

5.1   Assessment of forecast skill using CCI and other SST datasets

IC3/BSC has performed a first set of seasonal forecast simulations with the EC-Earth v3.1 model starting in May and November for four months for the hindcast period 1993 until 2009. The model is run at highest model resolution T511ORCA0.25 corresponding to approximately 40 km in the atmosphere and 25 km over the ocean.

Some evaluations of the model simulations have been done using either the CCI SST as a reference data set or other commonly used reference data sets. The comparisons shown here are focused on the ENSO prediction skill and the SST climatology.

ENSO prediction skill:

The correlations between observed and forecasted SSTs starting in May, averaged over the Niño 3.4 region and the 1993-2009 period, are reported in Figure 5.1. The correlations are shown for four different reference data sets, i.e. ERA-Interim, ERSST, HadlSST and CCI.

CMUG Phase 2 Deliverable

Reference:	**D4.1: MIP Impact Assessment**
Due date:	**30 June 2017**
Submission date:	**30 June 2017**
Version:	**3**

Correlation coefficients differ substantially between the different observations and CCI is within the spread of different observations. Most notable difference to other data sets occurs in May, where all other data sets agree strongly.
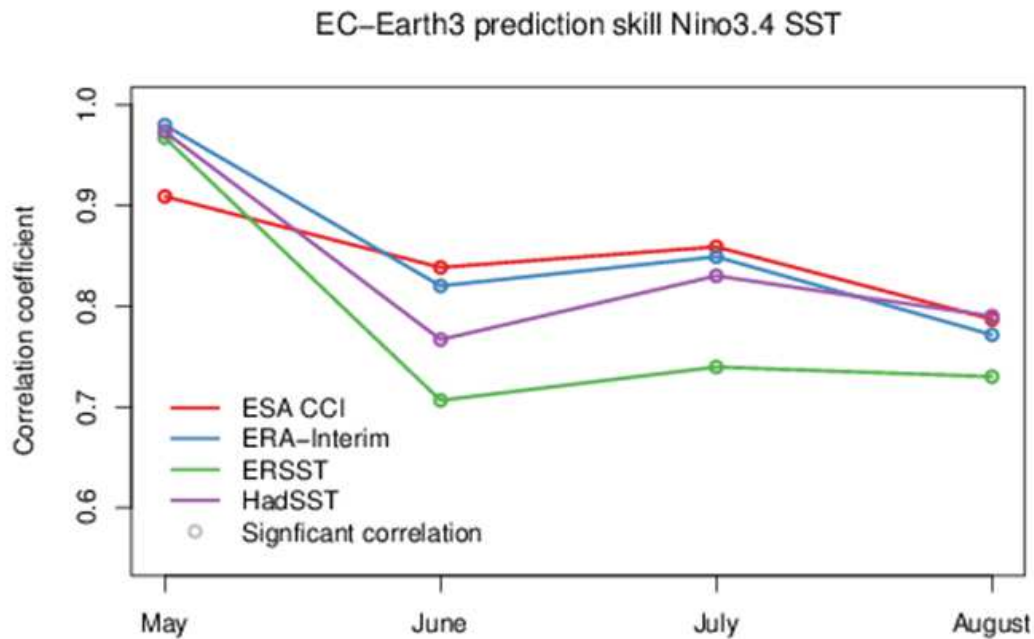

Figure 5.1: Correlations between observed and forecast SSTs starting in May, averaged over the Niño 3.4 region and the 1993-2009 period.

Climatological SST

Summer Sea-surface temperatures (SST) bias for the forecasts averaged over the 1993-2009 period and using the native model resolution, are shown in Figure 5.2. The reference data set is the CCI SST product. Validation at a resolution of 0.25° is so far only possible with this data set. Comparison to other data sets reveals a very similar pattern of SST biases (bottom row, left ERA-Interim and right HadlSST) with largest differences over the North Pacific.

CMUG Phase 2 Deliverable

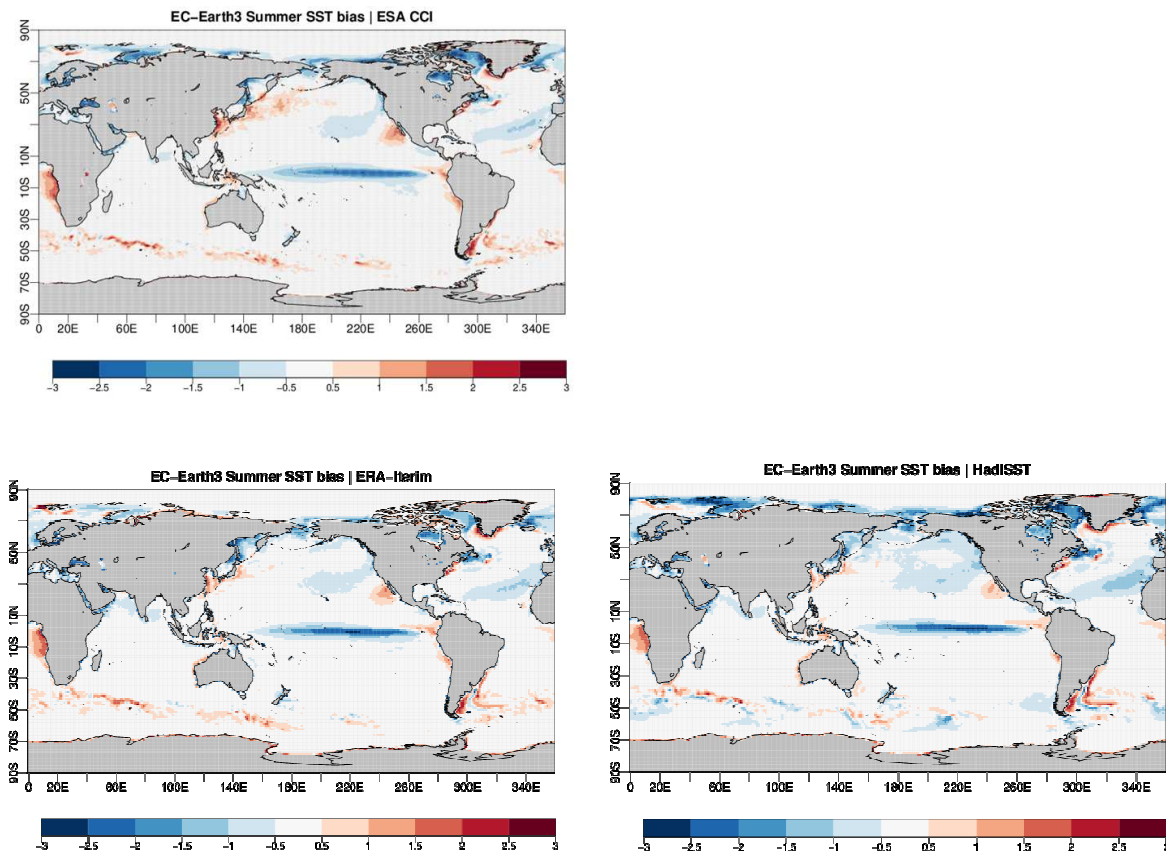|	
Reference:	**D4.1: MIP Impact Assessment**
Due date:	**30 June 2017**
Submission date:	**30 June 2017**
Version:	**3**

Figure 5.2: Summer Sea Surface Temperatures (SSTs) bias for the EC-Earth seasonal forecasts starting the 1ˢᵗ of May and averaged over the period 1993-2009. The reference data sets are the CCI SST (top), ERSST (bottom left) and HadSST (bottom right).

New sets of high-resolution seasonal prediction hindcasts with 25 km in the ocean and 40 km in the atmosphere have been then verified against multiple sets of observational references to understand how the forecast skill varies with the choice of reference data. The hindcasts cover the period of 1993 to 2009 predicting summer (JJA) and (DJF) respectively by initializing ten ensemble members on the 1st of May and November. The experiments have been carried out with the coupled Earth system model EC-Earth 3.1 (Hazeleger et al., 2010) using for the initialization of the ocean component Glorys2v1 (Ferry et al., 2010), ERA-Interim for the atmosphere (Dee et al., 2011), ERA-Land (Balsamo et al., 2015) for the land-surface and sea-ice initial conditions from Guemas et al.(2014).

The analysis focused in evaluating prediction skill measured by the ensemble mean temporal correlation of seasonal mean sea-surface temperature (SST) and sea-ice extent (SIE) using different observational datasets. Such an analysis can only be carried out with climate prediction experiments as non-initialized model integrations will not represent the same inter-annual variability as the one observed and atmosphere-only AMIP experiments are specifically forced by SST and SIE and hence do not allow for an independent evaluation of the observational references. The correlation analysis uses different sets of observations. For

CMUG Phase 2 Deliverable

Reference:	**D4.1: MIP Impact Assessment**
Due date:	**30 June 2017**
Submission date:	**30 June 2017**
Version:	**3**

SST we have used the products: CCI analysed v1.0 (Merchant et al., 2014), HadISST v.1.1 (Rayner et al., 2003), ERA-Interim (Dee et al., 2011), ERSST v.3b (Xue et al., 2003) and ERSST v.4 (Liu et al., 2014). For sea-ice extent: CCI SSM/I (Ivanova et al., 2014), HadISST v.1.1 (Rayner et al., 2003), OSI-SAF (Eastwood et al., 2011), COBE2 (Hirahara et al., 2014), NSIDC (Fetterer et al., 2016).
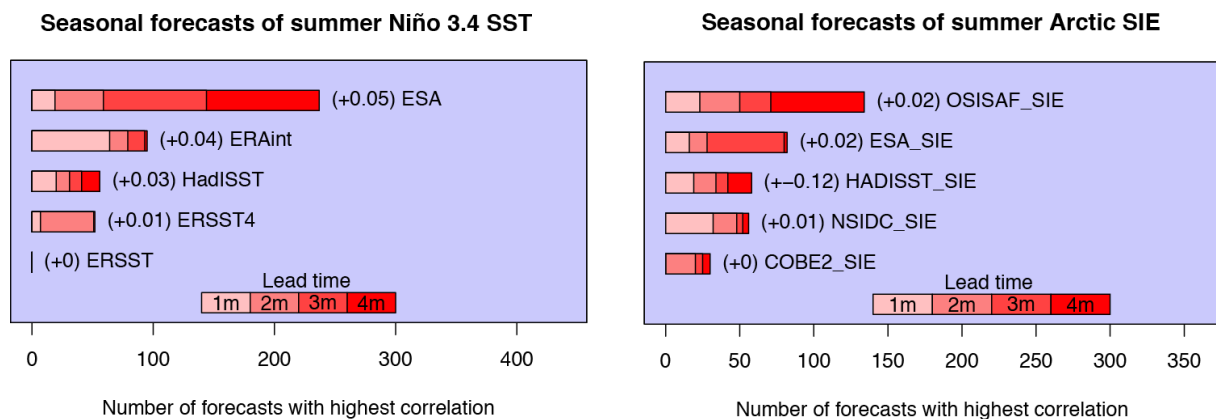

Figure 5.3: Numbers of forecasts with highest correlation when using different observations for Niño 3.4 SST or Arctic SIE using experiments and observations summarized in section 2a and b, respectively. Each bar is divided into the number of counts for each forecast lead-time (May - August) and brackets denote the average correlation increase due to a different dataset. ESA CCI and for OSI-SAF for SIE stand out as the observations providing systematically higher correlation skill.

As reported above the correlation skill of the EC-Earth high-resolution hindcast is systematically higher with ESA CCI for SSTs over the El Niño Southern Oscillation (ENSO) region Niño3.4 compared to other products. The analysis has therefore been extended to gain confidence of the result using an additional set of of climate model prediction systems from the North American Multi-Model Ensemble (http://www.cpc.ncep.noaa.gov/products/NMME/) for the same period and prediction of seasons but with varying resolution (all other models have a lower resolution). The Figure 5.3 shows a synthesis of the correlation skill across different products for SST and SIE by counting the number of times a single ensemble member reaches the highest correlation with one of the five products. The figure shows that for SST ESA CCI and for SIE OSI-SAF provide systematically higher correlation skill even if considering multiple models. The result has further been found to be very unlikely random.

Since the result is particularly striking for SST it has been extended spatially to assess its robustness beyond the Niño 3.4 region. Figure 5.4 shows the equivalent analysis of Figure 5.1 but depicting at each grid-point only the observations leading to the highest correlation (the observations with the longest bar in figure 5.3). The figure shows that the result is spatially inhomogeneous but that on average (33% of grid points) ESA-CCI provides the highest correlation also when considering the global oceans. Regions of intense ship traffic as the North Atlantic and North Pacific indicate that observations relying on in-situ measurements might be more accurate in these regions. The results are in review in Science Reports under the title "Utilizing climate models to estimate the quality of global observational data sets".

CMUG Phase 2 Deliverable

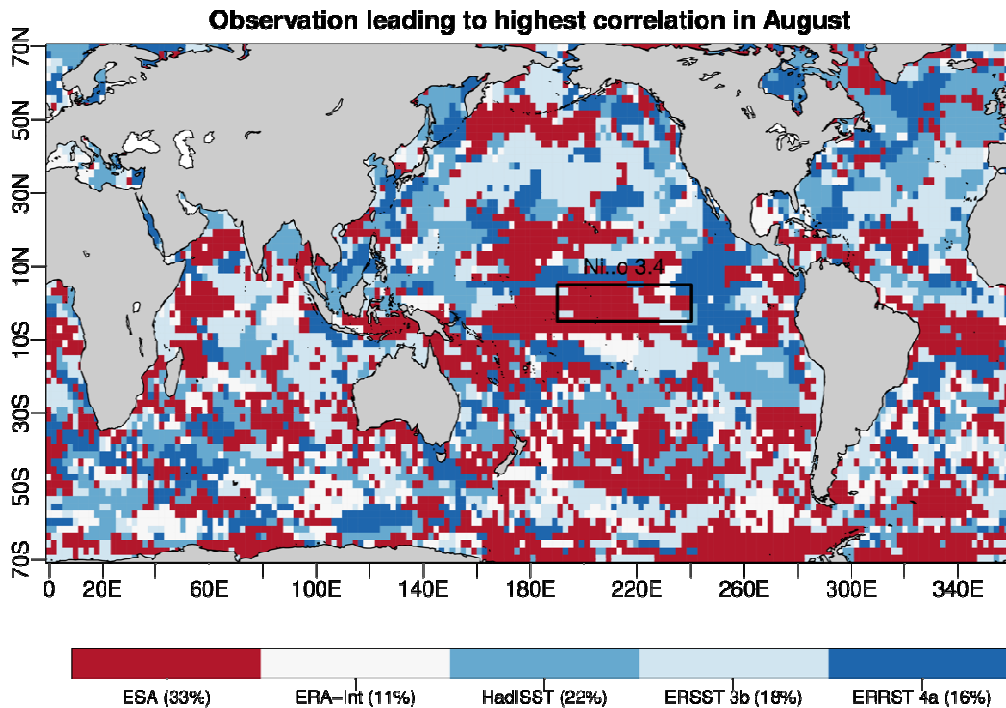|	
Reference:	**D4.1: MIP Impact Assessment**
Due date:	**30 June 2017**
Submission date:	**30 June 2017**
Version:	**3**

Figure 5.4: Spatial distribution of observational reference quality. For each grid point, we display the observational reference that correlates best with most of the forecasts. We show data only in grid points where at least one forecast achieves a significant correlation with one observational reference The black box is the Niño3.4 region. Regions above 70°N or below 70°S are not considered, as these regions are usually ice-covered. The percentages below the color bar indicate the fraction of the oceans covered by each color.

5.2 Assessment of forecast skill using observational uncertainties

At BSC, seasonal forecast verification practice has been enhanced to account for observational uncertainties provided by the CCI sea-surface temperature (SST) data. More specifically, the uncertainty provided by CCI SST is compared to the uncertainty derived from alternative observational references (ORs) of SSTs and to other sources of uncertainty in verification in order to assess its relevance. Figure 5.5 shows the correlation skill of Niño3.4 SSTs for predictions initialized in May predicting the consecutive four months (May-August). The correlation skill is accompanied with the uncertainties in the correlation skill shown as coloured areas around the sample estimate (dashed line). The uncertainty is decomposed into the observational uncertainty, the uncertainty originating from a limited ensemble size and the uncertainty from verifying the predictions for a limited period, constrained by the length of the CCI SST record (1992 - 2010). This analysis tells us two things: (1) the observational uncertainty can be an important source of uncertainty for the verification of seasonal predictions and current practice which does not account for these uncertainties should be revisited (2) the verification uncertainty is dominated by the length of CCI SST record; increasing the length of the record might hence reduce the uncertainty in model-observation comparison more than efforts devoted to reduce observational uncertainties.

CMUG Phase 2 Deliverable

Reference: **D4.1: MIP Impact Assessment**
Due date: **30 June 2017**
Submission date: 30 June 2017
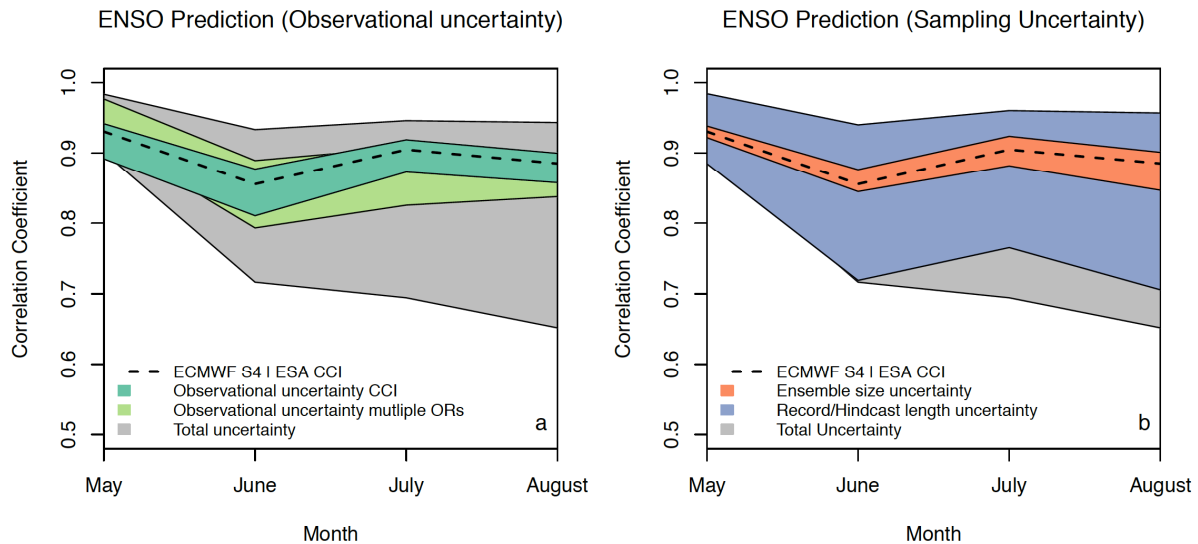**Version:**   **3**

Figure 5.5: Sub-seasonal to seasonal forecast skill of ECMWF S4 (10 members) with respect to SST CCI (dashed line). The areas show the 5-95% percentile range of the bootstrapped (10^6 samples) uncertainty sources around the sample correlation skill for (a) the uncertainty in the observations assessed using the SST CCI propagated uncertainty (l = 1000 km and t= 10 days) and the ensemble of different ORs and for (b) the sample uncertainty due to a limited ensemble size and record length of the SST CCI dataset. The grey area shows the total uncertainty obtained by resampling all sources at the same time

Observational uncertainties do not only increase the uncertainty in the forecast quality assessment of seasonal predictions but also systematically impact the skill. Noise in the observations decrease the correlation skill (Massonnet et al., 2016) and observational uncertainties lead therefore to an underestimation of the deterministic prediction skill of seasonal predictions. Figure 5.6 shows an estimate of how much skill is lost in seasonal SST predictions due to the uncertainties in the CCI SST record using the correction for attenuation (Spearman 1904). The figure shows that correlation skill is underestimated by more than 0.2 in various areas, which is highly relevant given that improvements in prediction skill due to improved model specifications is usually of a similar if not smaller magnitude (Prodhomme et al., 2016).

CMUG Phase 2 Deliverable

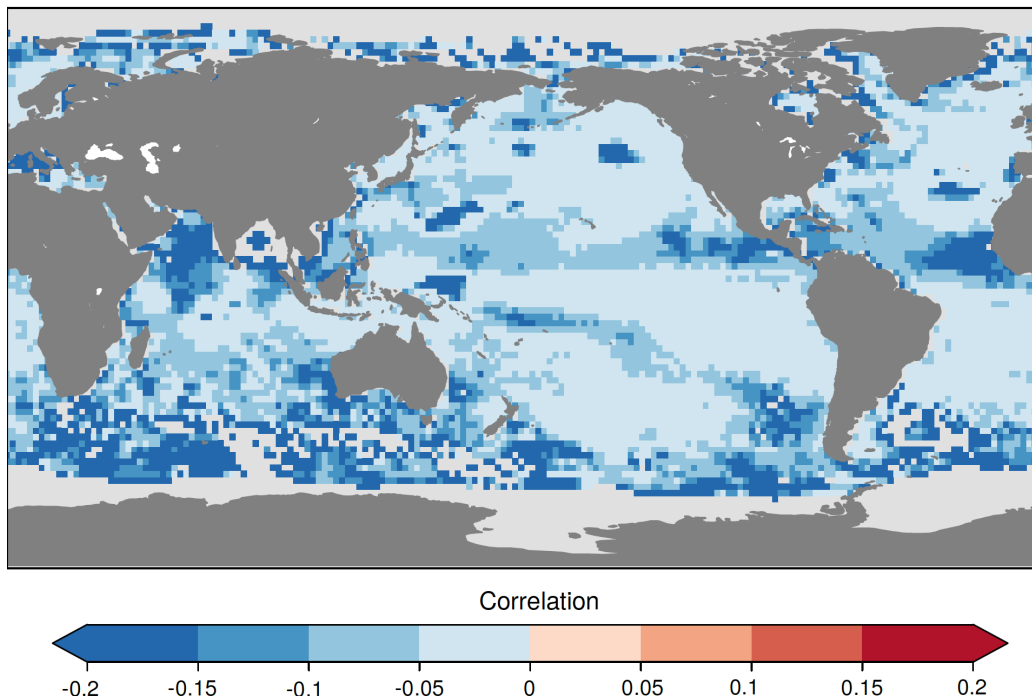|	
Reference:	**D4.1: MIP Impact Assessment**
Due date:	**30 June 2017**
Submission date:	**30 June 2017**
Version:	**3**

Lost skill due to observational uncertainty

Figure 5.6: Reduction of correlation skill in ECMWF S4 due to the observational uncertainty for the prediction of the month of August (initialized in 1st of May) estimated using the correction for attenuation (Spearman 1904). The observational uncertainty is estimated by propagating SST CCI uncertainties to monthly means in each grid-point. Grid-points in grey denote areas where the observational uncertainty is larger than the interannual variability of the SST CCI and where as a consequence no correction for attenuation can be calculated.

6. Discussion and conclusion

As a conclusion of the CC4MIP simulations, the analysis of the 5 member ensembles of simulations performed with T127 model version shows a slight but significant impact SST differences between the CCI and the AMIP datasets. Differences generally are not exceeding 0.1 to 0.2 K but the warmer temperature in the western tropical Pacific are sufficient to explain a significant increase of convective precipitation in the same region (about 10% of increase). Colder temperatures in the Indian Ocean have also an impact on the summer Indian monsoon. This is confirmed with the higher resolution simulations that also exhibit in boreal winter a circulation pattern at higher latitudes that resembles to a well-known teleconnexion with the western tropical Pacific. Conversely, we argue that the small differences in sea ice concentration between CCI and AMIP, particularly located in the marginal ice zone, seem not to have a significant impact on the simulated climate in spite of the high resolution of the analysed simulation. A complete demonstration would however require further investigation that could profit from similar CCI4MIP simulations performed with other atmospheric general circulation models.

Verification of seasonal climate prediction using ESA CCI observations and other observational datasets for the same variables reveals that forecast varies systematically, and robustly across multiple climate models, depending on which observational dataset is used. For SST we find that ESA CCI yields on average the highest forecast correlation which implies that the observational noise is smaller in ESA CCI compared to other SST products. The analysis presents a new paradigm of utilizing climate model prediction to estimate the quality of global observational data sets.

First results which make use of the CCI SST uncertainty in model-observation intercomparison reveal a large research area which has hardly been explored. Advancing our practice to account uncertainties for both models and observations will likely impact our future understanding of the level of state-of-the-art seasonal forecast skill but also climate model capabilities in general.

During the course of the project a discussion between CMUG partners (in particular SMHI) and CCI ice experts lead to the conclusion that including all signals (maybe marking certain areas as uncertain) but otherwise providing the data as they are is not a good solution from the climate modeller's perspective. Satellite groups should contain more knowledge over the "real world" sea ice conditions as modelling groups. Thus, it would be preferable if satellite groups provide their best estimate of the sea ice conditions instead leaving modelling groups to develop own algorithm to post-process the CCI data to make them usable for modelling activities. This would also lead to a large number of different "CCI"-like data sets. This was put in application since the version 2 of the sea ice concentration data set provided by the sea ice team includes both the raw variable that may exhibit some unrealistic values and a filtered variable but that might have the drawback of underestimating the sea ice concentration in marginal ice zones. This is this one that was used in the high resolution CCI4MIP simulation.

A more general point overcoming the specific context of the uncoupled AMIP simulations or the relatively short term seasonal forecast simulations is that climate models show huge variations over time. Ocean circulation features like the AMOC and related ocean heat transports can vary on multi-decadal time scales and affect also sea ice on these time scales. Since global climate models used in non-initialized coupled simulations do not reproduce the climate of certain years (e.g. year 2000) but only a climate that is representative for the external forcings (top of the atmosphere solar radiation, greenhouse gas concentrations, aerosol concentrations,…) of this year, very long data sets are needed to evaluated climate models. In this context often 30 years are mentioned but this is the lower limit given the fact that many ocean quantities vary on 50-80 year time scales.

7.   References

Balsamo, G., C. Albergel, A. Beljaars, S. Boussetta, E. Brun, H. Cloke, D. Dee, E. Dutra, J. Muñoz-Sabater, F. Pappenberger, P. de Rosnay, T. Stockdale, and F. Vitart, 2015 : ERA-Interim/Land: a global land surface reanalysis data set, Hydrol. Earth Syst. Sci., 19, 389-407, doi:10.5194/hess-19-389-2015.

Barsugli, J. J., & Sardeshmukh, P. D. (2002). Global atmospheric sensitivity to tropical SST anomalies throughout the Indo-Pacific basin. *Journal of Climate*, *15*(23), 3427-3442.

Dee, D. P., S. M. Uppala, A. J. Simmons, P. Berrisford, P. Poli, S. Kobayashi, U. Andrae, M. A. Balmaseda, G. Balsamo, P. Bauer, P. Bechtold, A. C. M. Beljaars, L. van de Berg, J. Bidlot, N. Bormann, C. Delsol, R. Dragani, M. Fuentes, A. J. Geer, L. Haimberger, S. B. Healy, H. Hersbach, E. V. Holm, L. Isaksen, P. Kallberg, M. Koehler, M. Matricardi, A. P. McNally, B. M. Monge-Sanz, J.-J. Morcrette, B. K. Park, C. Peubey, P. de Rosnay, C. Tavolato, J.-N. Thepaut, and F. Vitart, 2011 : The ERA-Interim reanalysis: configuration and performance of the data assimilation system. Q. J. R. Meteorol. Soc. 137: 553 – 597.

Ferry, N., L. Parent, G. Garric, B. Barnier, N. C. Jourdain and the Mercator Ocean team, 2010: Mercator Global Eddy Permitting Ocean Reanalysis GLORYS1v1: Description and Results. Mercator Ocean Quarterly Newsletter, 36, 15-27

Hazeleger, W., C. Severijns, T. Semmler, S. Ştefănescu, S. Yang, X. Wang, K. Wyser, E. Dutra, J. M. Baldasano, R. Bintanja, P. Bougeault, R. Caballero, A. M. L. Ekman, J. H. Christensen, B. van den Hurk, P. Jimenez, C. Jones, P. Kållberg, T. Koenigk, R. McGrath, P. Miranda, T. Van Noije, T. Palmer, J. Parodi, T. Schmith, F. Selten, T. Storelvmo, A. Sterl, H. Tapamo, M. Vancoppenolle, P. Viterbo, and U. Willén, 2010 : EC-Earth: A Seamless Earth-System Prediction Approach in Action. Bulletin of the American Meteorological Society, 91(10), 1357–1363.

Hewitt C, S. J. Mason, and D. Walland, 2012 : The global framework for climate services. Nature Climate Change, 831–832.

Hirahara, S., M. Ishii, and Y. Fukuda, 2014 : Centennial-scale sea surface temperature analysis and its uncertainty. J. Climate, 27, 7-75.

Hurrell, J.W., J. J. Hack, D. Shea, J. M. Caron, and J. Rosinski, 2008: A New Sea Surface Temperature and Sea Ice Boundary Data set for the Community Atmosphere Model. J. Climate, 21, 5145–5153, doi: http://dx.doi.org/10.1175/2008JCLI2292.1

Ivanova, N., T. Lavergne, L. T. Pedersen, and E. Rinne, 2014 : ESA-CCI Sea Ice ECV Project D3.6 Algorithm Theoretical Basis Document (ATBD) version 2.0, issue 1.0, ESA SICCI project report SICCI-ATBDv2-13-09, May 13 2014.

Liu, W., B. Huang, P. W. Thorne, V. F. Banzon, H. M. Zhang, E. Freeman, J. Lawrimore, T. C. Peterson, T.M. Smith, and S; D. Woodruff, 2015. Extended reconstructed sea surface temperature version 4 (ERSST. v4): Part II. Parametric and structural uncertainty estimations. J. Climate, 28(3), 931-951.

Massonnet, F., O. Bellprat, V. Guemas, and F. J. Doblas-Reyes, 2016: Using climate models to estimate the quality of global observational data sets. Science, 354,452–455.

Merchant, C.J., O. Embury, J. Roberts-Jones, E. Fiedler, C. E. Bulgin, G. K. Corlett, S. Good, A. McLaren, N. Rayner, S. Morak-Bozzo, and C. Donlon, 2014 : Sea surface temperature datasets for climate applications from Phase 1 of the European Space Agency Climate Change Initiative (SST CCI). Geoscience Data Journal, 1(2), 179-191.

Merchant, C., and P. Spink. 2013 : SST CCI Product User Guide. http://www.esa-sst-cci.org/sites/default/files/Documents/public/SST_CCI-PUG-UKMO-001_Issue-3-signed-accepted.pdf

Palmer, T. N., and Mansfield, D. A. (1984). Response of two atmospheric general circulation models to sea-surface temperature anomalies in the tropical east and west Pacific. *Nature*, *310*(5977), 483-485.

Prodhomme, C., L. Batt, F. Massonnet, P. Davini, O. Bellprat, V. Guemas, and F. J. Doblas-Reyes, 2016: Benefits of increasing the model resolution for the seasonal forecast quality in EC-Earth. Journal of Climate, 29, 9141–9162.

Rayner, N.A., D.E. Parker, E.B. Horton, C.K. Folland, L.V. Alexander, D.P. Rowell, E.C. Kent, and A. Kaplan, 2003 : Global analyses of sea surface temperature, sea ice, and night marine air temperature since the late nineteenth century. J. Geophys. Res.Vol. 108, No. D14, 4407, DOI: 10.1029/2002JD002670.

Révelard, A., 2017 : Influence de la variabilité du Kuroshio, de l'Oyashio, et de l'Oscillation décennale du Pacifique sur la circulation atmosphérique nord pendant la saison froide. Thèse de doctorat de l'Université Pierre et Marie Curie (Paris VI), 136pp.

Smith, T.M., R.W. Reynolds, T.C. Peterson, and J. Lawrimore 2007: Improvements to NOAA's Historical Merged Land-Ocean Surface Temperature Analysis (1880-2006). In press. Journal of Climate.

Sørensen, A., and T. Lavergne, 2017: Sea ice CCI Product User Guide v1.0. http://data.ceda.ac.uk/neodc/esacci/sea_ice/docs/SICCI_P2_SIC_PUG_D3.3_Issue_1.0.pdf

Spearman, C., 1904: The Proof and Measurement of Association between Two Things. The American Journal of Psychology, 15, 72–101.

Taylor, K. E., D. Willamson, and F. Zwiers, 2015 : AMIP surface temperature and sea ice concentration boundary conditions. http://www-

pcmdi.llnl.gov/projects/amip/AMIP2EXPDSN/BCS/#BM2___Construction_of_the_AMIP_2
_Boundar.

Voldoire, A., E. Sanchez-Gomez, D. Salas y Mélia, B. Decharme, C. Cassou, S. Sénési, S. Valcke, I. Beau, A. Alias, M. Chevallier, M. Déqué, J. Deshayes, H. Douville, E. Fernandez, G. Madec, E. Maisonnave , M.-P. Moine, S. Planton, D.Saint-Martin, S. Szopa, S. Tyteca, R. Alkama, S. Belamari, A. Braun, L. Coquart, F. Chauvin, 2013 : The CNRM-CM5.1 global climate model: description and basic evaluation. Climate Dynamic, Volume: 40, Issue: 9-10, Special Issue: SI, Pages: 2091-2121, DOI: 10.1007/s00382-011-1259-y, Published: MAY 2013.

Xue, Y., T. M. Smith, and R. W. Reynolds, 2003: Interdecadal changes of 30-yr SST normals during 1871-2000. J. Climate, 16, 1601-1612.